

Article

Application of the Ground Penetrating Radar (GPR) and Electromagnetic (EM34-3) Geophysical Tools and Sedimentology for the Evaluation of the Subsurface of Sites Earmarked for Aquaculture Ponds in the Amazon Region of Northern Brazil

Ramon Wagner Torres Pena , Pedro Andrés Chira Oliva *  and Fernando Araújo Abrunhosa

Coastal Studies Institute (IECOS), Federal University of Pará, Alameda Leandro Ribeiro s/n, Aldeia, Bragança 68600-000, Brazil; ramon.pena@braganca.ufpa.br (R.W.T.P.); faraujo@ufpa.br (F.A.A.)

* Correspondence: chira@ufpa.br

Abstract: The present study evaluated the application of Ground Penetrating Radar and Electromagnetic Induction geophysical tools combined with sedimentology for the description of the subsurface of sites destined for the installation of ponds for an extensive freshwater fish farming system. Two areas with similar topographic characteristics (flat land near bodies of water) were investigated in the Amazon region of northern Brazil: Area 1—the future site of an aquaculture research center, and Area 2—an established fish farming operation. These tools performed well in the evaluation of the suitability of the terrain for the installation of aquaculture ponds. The application of these tools can, thus, be recommended for aquaculture projects, given that it provides advanced knowledge on the characteristics of the local soils, which is extremely important to guarantee the sustainability of any aquaculture operation. These data can help minimize the environmental impacts of the process, while maximizing the economic returns to the installation of an aquaculture operation.

Keywords: Ground Penetrating Radar; electrical conductivity meter; excavated nurseries; apparent conductivity; groundwater



Citation: Pena, R.W.T.; Oliva, P.A.C.; Abrunhosa, F.A. Application of the Ground Penetrating Radar (GPR) and Electromagnetic (EM34-3) Geophysical Tools and Sedimentology for the Evaluation of the Subsurface of Sites Earmarked for Aquaculture Ponds in the Amazon Region of Northern Brazil. *Appl. Sci.* **2023**, *13*, 11107. <https://doi.org/10.3390/app131911107>

Academic Editors: Deshan Feng, Xun Wang and Bin Zhang

Received: 18 August 2023

Revised: 23 September 2023

Accepted: 25 September 2023

Published: 9 October 2023



Copyright: © 2023 by the authors. Licensee MDPI, Basel, Switzerland. This article is an open access article distributed under the terms and conditions of the Creative Commons Attribution (CC BY) license (<https://creativecommons.org/licenses/by/4.0/>).

1. Introduction

Aquaculture, or fish farming, refers to the cultivation of fresh- or saltwater organisms and is a well-developed economic activity that is accelerating rapidly throughout the world [1,2]. Fish farming can contribute to the domestic output of fishery products, provide an important source of income for many smallholders, other landowners and their local communities, through their direct involvement in the value chain (production, processing, and sale), as well as offering employment opportunities [3,4]. Aquaculture and fisheries are the fastest-growing food production systems around the world and their importance for food security and global nutrition in the twenty-first century is recognized increasingly by authorities such as [5–7].

The installations required for the production of fish—either ponds or net enclosures—represent the principal investment in any aquaculture operation. However, the costs of the construction of ponds or the implantation of other structures may vary considerably according to factors such as the characteristics of the site (climate, topography, type of soil, vegetation cover, and drainage requirements), the configuration of the infrastructure, and the methods employed to install the operation. These costs can, nevertheless, be minimized through the adequate planning of the different stages of the installation process [8].

Before making any investments or making decisions on the installation of fish farming infrastructure, it is extremely important to carefully evaluate the site earmarked for

development. In particular, the technical conditions of the site should be verified, in addition to the most adequate procedures to ensure the integrity of the local environment, in line with the existing legislation. Many sites are totally inadequate for fish farming due to factors that range from the high permeability of the soil, the risk of floods and other environmental impacts, and an inadequate supply of water to a lack of access roads or access to a power grid [9].

The selection of an appropriate site is fundamentally important here and adequate site selection will reduce the possible environmental impacts of the operation and the potential conflicts of this activity with the use of other resources and the sustainable development of aquaculture activities [6,7,10]. This will also guarantee an increase in economic returns [11–13].

1.1. Motivation

Aquaculture has grown considerably in Brazil over the past few decades, in line with global trends, to become a valuable source of income and employment [2,14]. In 2022, Brazil produced 860,355 tons of farmed fish, based on data from the Brazilian Pisciculture Association. This represents an increase of 2.3% over the 841,005 tons produced in 2021. Since 2014, in fact, the annual production of farmed fish in Brazil has increased by almost half (281,555 tons or 48.6%) [15]. The majority of these fish are produced by smallholders in ponds with an area of less than 2 ha, a pattern similar to that observed in a number of prominent fish-farming countries in Asia [16].

In addition to the possibility of generating a profit from aquaculture, smallholders are encouraged to invest in the production of aquatic organisms, such as fish, shrimp, frogs, oysters, and algae, by the demand from local and regional markets, the availability of water, land (including lakes, reservoirs, and coastal environments), and, in most Brazilian states, the access to raw materials. The vast majority of these producers initiate their aquaculture operations without any planning or preliminary survey, however, which has led many to abandon or downsize their operations [11]. There are a number of other weak links in the chain of production, such as the transfer of technology, technical support, the availability of credit, government policy, and the regulation of the sector [16].

One other problem observed frequently in Brazil is the inadequate evaluation of the subsoil of sites earmarked for the excavation and construction of fish-farming ponds. A lack of adequate technology for the systematic assessment of the subsoil of sites earmarked for fish ponds has led to the failure of some projects, due to the instability of the infrastructure. Given the resources required to collect and analyze samples, and the delay in obtaining the final results, the need for a detailed on-site assessment may limit the viability of fish farming for many small- to medium-sized producers.

Few rural landowners in the northern Brazilian state of Pará—in particular in the geographic region of Bragança—are aware of the technology available to survey the subsoil of terrains earmarked for fish farming ponds and this lack of an adequate database has caused the failure of many projects. The reasons for failure range from inappropriate decision making on the types of terrain and aquaculture system to be used to the construction of inadequate installations. While reliable data on the structure of the subsoil are essential for the success of any aquaculture project, the high costs of obtaining and analyzing these data, as well as the time required to obtain the results, may represent a major limitation in many cases.

1.2. Contributions

Until recently, the selection of sites has tended to be driven primarily by the suitability of the local environment for the target species and by historical inertia in areas where aquaculture is well-established [17].

Over the past three decades, a number of studies have described the use of different types of geotechnology, such as Geographic Information Systems (GIS), Remote Sensing (RS), Global Navigation Satellite System (GNSS), and digital cartography, for the selection

of sites for aquaculture ponds [18]. Remote Sensing (RS) and GIS are considered to be important tools for the evaluation of areas destined for aquaculture (e.g., [19–21]).

Geophysical tools are one other valuable option for the description of the quality of soils. This technology is non-invasive, non-destructive, and has excellent spatio-temporal resolution (e.g., [22–24]), and can provide valuable information on the characteristics of the subsoil, including its lithology, stratigraphy, bedrock, water table, and the presence of depressions, faults, and fractures (e.g., [25–38]).

Electrical and electromagnetic methods are the techniques used most frequently (e.g., [22,23,39–41]). The most important of these methods in the context of the present study are Ground Penetrating Radar (GPR) and Electromagnetic Induction (EMI), which have been employed successfully in studies of soils to determine their properties and spatial-temporal variability [42].

In the present study, the application of two geophysical tools (GPR and EMI) permitted the systematic evaluation of the subsoil of sites earmarked for the installation of aquaculture ponds. The acquisition and operation of the GPR and EMI do not demand an excessive investment and are cost-effective, given their durability and low maintenance costs, while also contributing to the preservation of the environment. The surveys can be conducted by teaching institutions, local administrations, government agencies that provide technical support in rural areas, and even farming cooperatives and associations. We combined these geophysical tools with the sedimentological analysis (rapid field tests) of the study terrains and present an important alternative approach for the verification of the viability of sites earmarked for the installation of fish farming ponds.

1.3. Organization

The present study was based on an approach that integrated direct and indirect methods of investigation. The indirect, electromagnetic methods used here were Ground Penetrating Radar (GPR) and Electromagnetic Induction (EM34-3), which were combined with two direct methods—sedimentological analyses and the Standard Penetration Test (SPT)—for the diagnosis of the characteristics of the subsoil of two potential aquaculture sites in the geographic region of Bragança, in northern Brazil.

The results of these analyses demonstrate that these analytical tools can be used successfully in an integrated approach for the evaluation of sites earmarked for aquaculture installations. These tools permit the systematic description of the terrain. The study provided essential data for the effective selection of terrains for fish-farming operations.

2. Materials and Methods

2.1. Study Area

The aquaculture sites evaluated in the present study (Figure 1) are located in the geographic region of Bragança, in northern Brazil [43]. Two areas with similar topographic characteristics (flat land near bodies of water) were investigated: Area 1 is a site at which the Northeastern Pará Aquaculture Center (CEANPA) is currently under construction in the municipality of Bragança ($1^{\circ}02'41.07''$ S, $46^{\circ}42'15.81''$ W), approximately 8 km from Bragança town center, and Area 2, which is a privately-owned, small-scale fish farm located in the municipality of Tracuateua ($0^{\circ}56'27.34''$ S, $46^{\circ}53'37.23''$ W).

The study area is located within the Bragança–Viseu basin, which has a tectonic trench delimited by normal (NW–SE) faults [44]. The thickness of the principal Cenozoic deposits found in this area was determined by its paleorelief, in combination with tectonic processes (e.g., [45–47]). The Cenozoic units found within this region are represented by the Pirabas Formation, the Barreiras and Post-Barreiras groups, and by modern sediments.

The local climatic cycle alternates between a rainy season, typically between December and May, and a dry (or less rainy) season, typically between June and November [48]. These values may vary considerably, however, in particular when influenced by long-term climate events, such as El Niño or La Niña [49].

The proposed method includes the following steps (Figure 2):

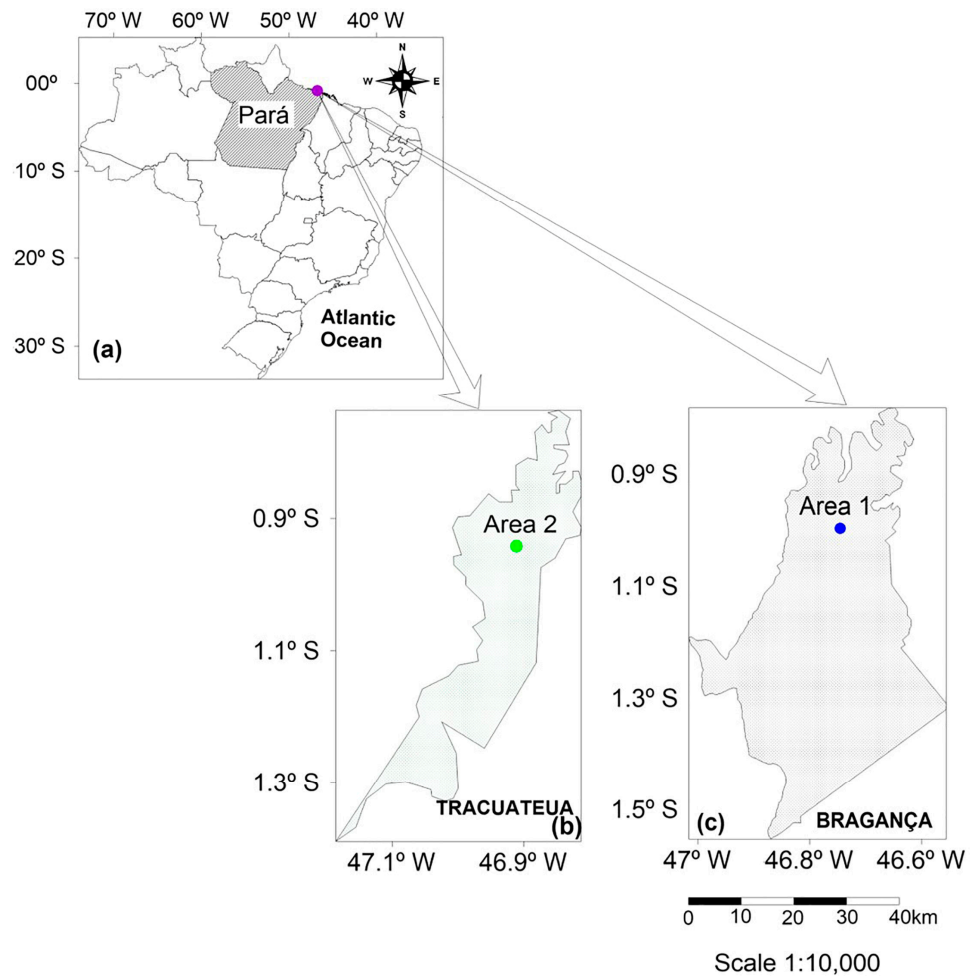


Figure 1. Study area: (a) Brazil showing the state of Pará (hatched area) and the location of the two study sites (blue and green dots) within the municipalities of Tracuateua (green shading) (b) and Bragança (black shading) (c).

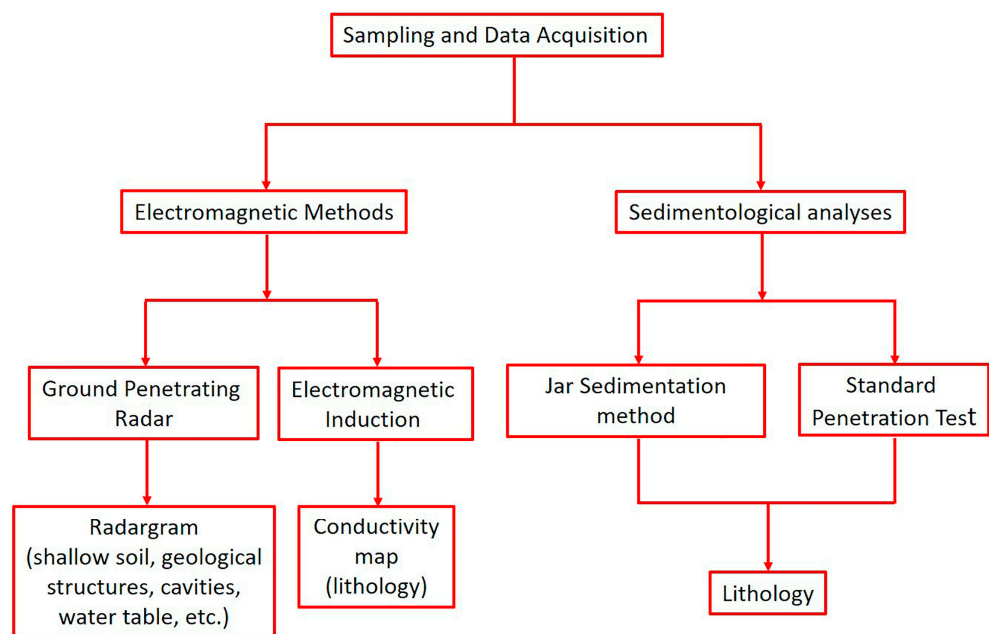


Figure 2. Flowchart of the methods employed in the present study.

2.2. Ground Penetrating Radar (GPR)

Ground Penetrating Radar is a non-destructive geophysical tool that uses high-frequency electromagnetic (EM) waves in the 10–1000 MHz range to survey subsurface structures. The propagation of an EMI signal depends on the frequency of the transmitted signal and the electrical properties (electrical conductivity, dielectric permittivity, and magnetic permeability) of the substrate.

A GPR survey provides an image of the subsoil along the study profile [29]. This tool can be applied in both natural and urban environments and can generate high-resolution images of features such as shallow soils and geological structures, as well as detecting buried and underground cavities, the water table, and archaeological artefacts. This type of radar emits short pulses at frequencies of between 10 and 1000 MHz, which are transmitted into the subsoil, where the propagation velocity (v) is controlled by the relative permittivity (dielectric constant, ϵ'_r) and conductivity (σ) of the substrate (see, e.g., [29,30,37,50]).

For low-loss geological materials, the electromagnetic field is propagated at a phase velocity of

$$v = \frac{c}{\sqrt{\epsilon'_r}} \quad (1)$$

where c = the propagation velocity of electromagnetic waves in a vacuum ($c \cong 0.3$ m/ns) and ϵ'_r = the dielectric constant of the substrate [38].

The most important determinants of the propagation of the electromagnetic wave through a given medium are its velocity and attenuation. When these waves travel through conductive material, the electromagnetic energy is lost in the form of heat through the electric current. This loss of energy is the attenuation that provokes a reduction in the depth of the penetration of the radar waves.

In rocks of high resistivity ($> 10^2$ ohm.m), the propagation velocity of the pulse is controlled primarily by ϵ'_r . Water has a dielectric constant of 80, while most dry geological materials have a dielectric constant of 4–8. Given this, the water content of the material has a strong influence on the propagation of a radar pulse [37,38].

The wavelength, λ (m), is given by

$$\lambda = \frac{c}{f \sqrt{\epsilon'_r}} \quad (2)$$

where f = the central frequency of the antennas.

The attenuation constant (α) is normally expressed as

$$\alpha = 1.636 \times 10^3 \frac{\sigma}{\sqrt{\epsilon'_r}} \quad (3)$$

in dB/m, where σ = the electrical conductivity ($\text{mS}\cdot\text{m}^{-1}$) [38].

2.3. Electromagnetic Induction (EMI)

Electromagnetic surveys are based on the measurement of electrical conductivity and the magnetic permeability derived from the materials found in the subsurface using electromagnetic fields that are induced naturally or artificially in the study terrain. One interesting feature of the electromagnetic method is that it does not require direct contact with the ground being surveyed [29,37]. The EMI method is rapid, non-invasive, and cost-effective, and is implemented using transmission (T_x) and receptor (T_r) coils, as described in detail by [22,39,51,52].

An alternating electrical current, which is produced by the transmission unit at a set frequency, passes through the transmission coil (T_x) to produce a primary, alternating magnetic field (H_p), which induces secondary electrical currents in the subsurface that generate a secondary magnetic field (H_s). Part of this magnetic field is captured by the receptor coil (T_r), which also receives part of the primary magnetic field through a reference cable. The

differences detected in the intensity, direction, and phase between these electromagnetic fields can be used to detect the presence of conductive bodies [51,53].

In general, the secondary magnetic field depends on the spacing of the coils (S), the operating frequency (ω), and the conductivity of the terrain (σ). However, when operating at low induction numbers, where the product $\omega\sigma S^2$ is less than 1000, the following equation can be employed [51]. These restrictions are incorporated into the EM 34-3 conductivity meter, in which the secondary magnetic field is defined by

$$\frac{H_s}{H_p} = \frac{i\omega\mu_0\sigma S^2}{4} \quad (4)$$

where H_s = the secondary magnetic field, H_p = the primary magnetic field, $\omega = 2\pi f$ (angular frequency), $i = \sqrt{-1}$, μ_0 = magnetic permeability of free space, σ = ground conductivity ($\text{mho}\cdot\text{m}^{-1}$), and S = intercoil spacing (m).

The electrical conductivity varies according to the type of soil or rock, porosity, permeability, the degree of saturation, and the electrochemical properties of the liquids found in the pores, which is the most important factor in many cases [51].

2.4. Standard Penetration Test (SPT)

The Standard Penetration Test (SPT) uses percussion drilling with circulating water to determine the characteristics of the soil of a terrain earmarked for the construction of buildings or other infrastructure. This test provides information on the compactness and consistency of the underground layers that make up the substrate, and determines the different types of subsoil and the depths at which they occur, the depth of the water table, and the penetration resistance index (N) at each meter of depth [54,55], which is necessary to determine the resistance of the soil.

The SPT is conducted in the field through the dynamic penetration of a standardized sampler, which is inserted into the different soil layers using an iron hammer. The SPT permits the collection of deformed samples of the subsoil to determine the local stratigraphy through the visual-tactile analysis of its distinct layers as far down as the depth reached by the probe.

2.5. Sampling and Data Acquisition

2.5.1. Acquisition of Data by GPR

The GPR data were acquired using a GSSI SIR 3000 GPR system (Salem, NH, USA), with 200 MHz and 400 MHz antennas. The GPR sections were acquired within a time window of 200 ns. The survey was georeferenced with a handheld GPS with Navigation Sensors (GPSMAP 64SX), Garmin Ltd. (Olathe, Kansas, U.S.A.). The acquisition system of the electromagnetic signals was bi-static, with a standard offset between the transmitter and receiver antennas.

The GPR was calibrated in an area adjacent to each fish-farming site, where a hole was excavated and a metal bar was inserted to a depth of approximately 50 cm to obtain a test profile and determine the propagation velocity of the electromagnetic waves using the hyperbole overlap method.

The GPR data were collected at this site (Area 1, Figure 3a) in March 2017. Four profiles were surveyed: AB (240 m in length, with readings being taken at intervals of 10 m), BC (60 m in length, 5 m intervals), CD (40 m in length, 5 m intervals), and EF (45 m in length, 5 m intervals).

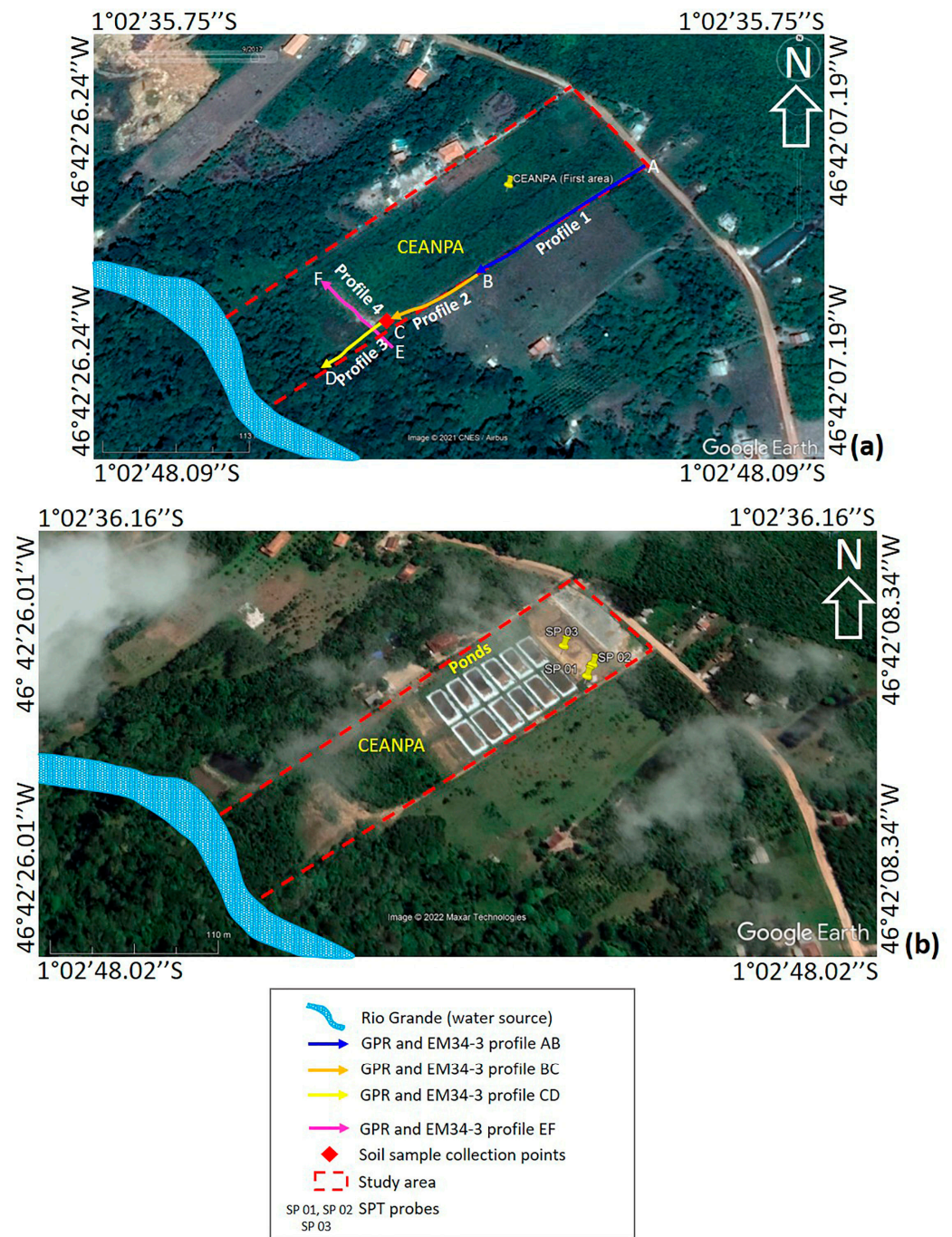


Figure 3. Area 1 (Bragança, Pará), on which an aquaculture research center (CEANPA) is under construction, showing the geophysical profiles (a) and the location of the ponds (b) (modified from [56]).

The privately-owned fish farm (Area 2, Figure 4) was also surveyed using GPR in March 2017. Two profiles were surveyed: AB (400 m in length and readings taken at intervals of 5 m) and CD (105 m in length, 5 m intervals). The terrain is flat.



Figure 4. Area 2 (Tracuateua, Pará): a privately-owned aquaculture facility (modified from [56]).

2.5.2. EMI Data Acquisition

The EM34-3 electrical conductivity meter is a two-man portable instrument with two dipole modes: the Horizontal Dipole (HD), in which the coil axes are arranged vertically and the potential survey depth is approximately 0.75 times the distance between the coils, and the Vertical Dipole (VD), in which the coil axes are arranged horizontally and the survey depth is approximately 1.5 times the distance between the coils. As mentioned above, the Tx-Rx coils may be arranged at intervals of 10 m, 20 m, or 40 m. Under ideal conditions, these intervals permit the investigation of depths of approximately 7.5 m, 15 m, and 30 m, respectively, in the HD mode, and 15 m, 30 m, or 60 m in the VD mode [51].

The EM34-3 electrical conductivity meter used in this study was an Electromagnetic Frequency (EMF) system developed by Geonics Limited (Mississauga, ON, Canada) for applications in Electromagnetic Induction. This apparatus is used as an alternative for electrical surveys that employ galvanic techniques to measure apparent electrical resistivity. The use of the EM34-3 permitted the rapid mapping of the conductivity of the subsurface of the study terrain [51].

The EM data were collected in March 2017. The apparent conductivity data were measured in $\text{mS}\cdot\text{m}^{-1}$. At one of the study sites (Area 2), the ponds had already been excavated to a depth of 1–2 m. We evaluated the data collected by the Horizontal Dipole (HD) with the coils spaced at 10 m intervals, which surveys depths of up to approximately 7.5 m [51]. The EMI surveys were run in the same directions as the GPR profiles (Figure 3).

2.5.3. Sedimentological Analyses of the Soil Samples

While the texture of the soil and its particle size can be analyzed by specialized laboratories, the soil texture was determined in the present study using a rapid field test. For this, 600 mL samples of soil were collected using an auger and 1 m deep trenches (Figures 3 and 4). The samples were labeled prior to the analysis, which had three steps:

- Two subsamples of approximately 300 mL of the soil were placed in two transparent 2 L jars (Jar Sedimentation Method);

- The samples were then ground up with a rod to eliminate the air trapped in the soil and record the volume of the material in the container;
- A total of 1500 mL of water was added to each container to homogenize the soil and dissociate all the particles present in the sample. After decanting for 24 h, the proportions of gravel, sand, silt, and clay present in the soil were determined and measured.

The successful implementation of fish-rearing ponds may depend on the quality of the soil [57,58]. These authors recommend that the soil should be impermeable, with at least 20% clay, to minimize the loss of water by infiltration, for which clayey or loamy soils are ideal. Reference [59] classified soils as being either sandy (0–16.0% clay), loamy (medium) (16.1–32.0% clay), clayey (32.1–60.0% clay), or very clayey (>60.0% clay).

2.5.4. Standard Penetration Test

The SPT was conducted following [54], as recommended by the Brazilian norms system (NBR). The test consisted of the dynamic penetration to 45 cm of a standard sampler by hitting it successively with a hammer weighing 65 kgf, which was allowed to fall freely from a height of 75 cm. The 45 cm of the insertion of the probe was divided into three sectors of 15 cm, with the number of strikes of the hammer necessary for the probe to penetrate each sector being counted. The penetration resistance index (N) is the sum of the number of strikes necessary to insert the probe into the final 30 cm, that is, the last two sectors of the probe.

The standardized sampler had an external diameter of 50.80 mm, internal diameter of 34.90 mm, and was inserted using lining tubes with an internal diameter of 66.50 mm and steel rods with an internal diameter of 25 mm and weight of 3 kgf.mL⁻¹. The perforation and collection of the deformed subsoil samples from the different depths of study Area 1 (Figure 3) were conducted in July, 2015 by the PLENO Architecture and Construction Company [60].

2.6. Data Processing

2.6.1. GPR

The noise in the electromagnetic signals recorded using the GPR in the present study was removed for analysis. The data were also edited, with spatial resampling and interpolation being applied to the traces. The data processing involved the following steps (e.g., [25–37,61–64]): static correction of zero-time, gain, time filtering (1D), and spatial filtering (2D), that is, background removal and moving average trace subtraction. The hyperbole overlap method was used for the time-depth conversion, by obtaining a propagation velocity of 0.092 m/ns.

2.6.2. EMI

The Golden Surfer software was used to process the EMI data and formulate the maps of conductivity. This processing had six steps: (i) Edition of the data spreadsheets; (ii) Importation of the data to the software; (iii) Interpolation of the data by triangulation; (iv) Formulation of initial conductivity maps; (v) Application of the color filters; (vi) Formulation of the final map of conductivity.

3. Results

3.1. Area 1

Two antennas (200 and 400 MHz) were tested in Area 1 (Bragança). The GPR prospection reached a depth of 8–9 m but with the occurrence of noise at depths of below approximately 1 m (Figure 5c,d). The AB profile (Figure 5a) revealed an abrupt depression at a depth of up to 4.5 m. A compact layer was also identified near the surface (0.25–0.5 m).

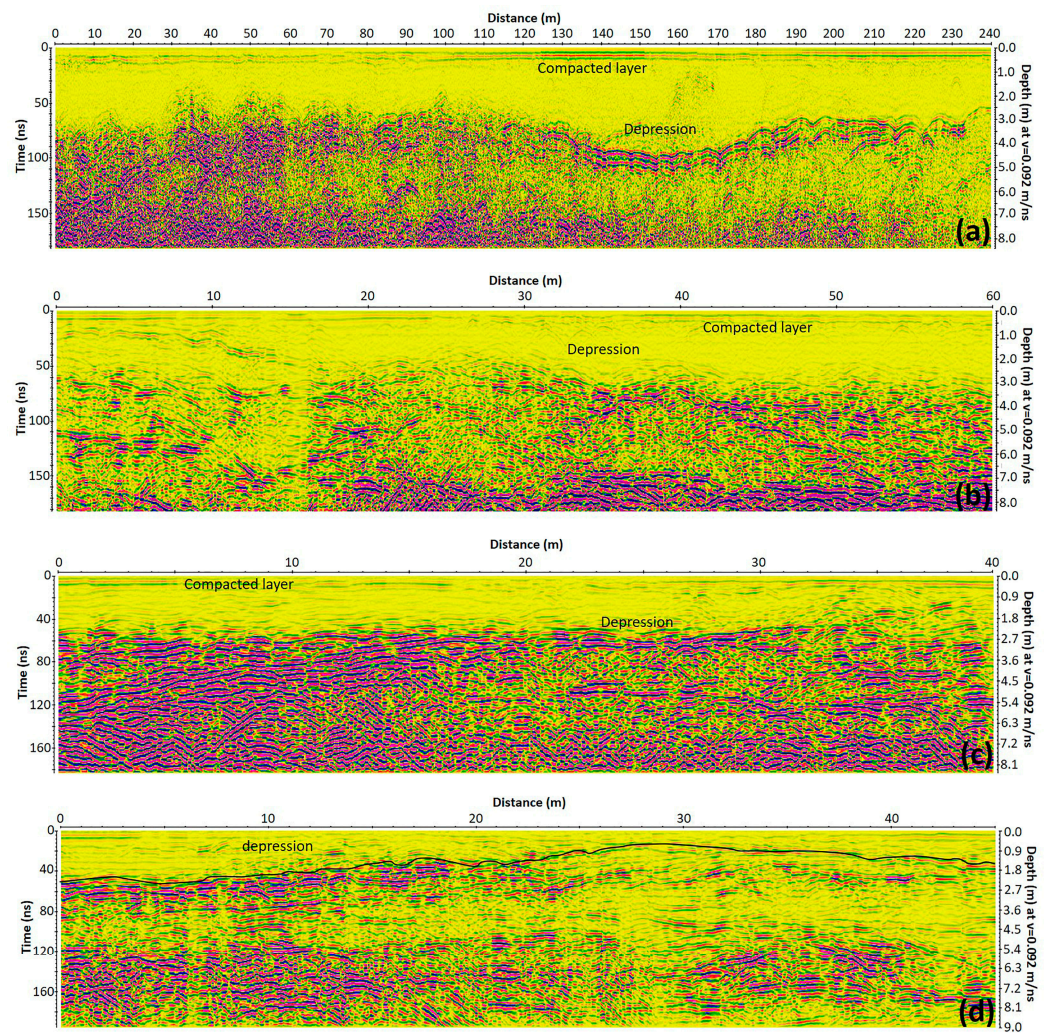


Figure 5. The GPR profiles (200 MHz antenna with a 200 ns time window) recorded in Area 1 (Bragança): (a) AB; (b) BC; (c) CD; (d) EF.

The BC profile (Figure 5b) revealed the same depression as the AB profile, extending to a depth of 3 m, and the same compacted layer (0.25–0.50 m). In the CD profile (Figure 5c), an abrupt depression was identified at a depth of 2.7 m. This profile was surveyed near a stream (Rio Grande), which runs perpendicularly to study Area 1 and is earmarked as the future source of water for the 12 fish-farming ponds excavated at this site (Figure 3b). The EF profile (Figure 5d) also identified an abrupt depression at a depth of up to 2.16 m. The yellow shading in the profiles shown in Figure 5 indicates the zones of low reflection, in which the electromagnetic wave has a low amplitude, due to the attenuation of the GPR signal, while the other colors indicate the zones with high reflection and high amplitude.

The apparent conductivity recorded in Area 1 was low, with values ranging from 3.5 to 17 $\text{mS}\cdot\text{m}^{-1}$ (Figure 6). This indicates the possible presence of a clayey subsoil [38]. The saturation of the substrate tends to increase its electrical conductivity, causing attenuation of the electromagnetic signal. The soils of the study area, in the municipality of Bragança (Pará), are yellow latosols which are derived from the clayey and sandy–clayey sedimentary substrates of the Barreiras formation [65].

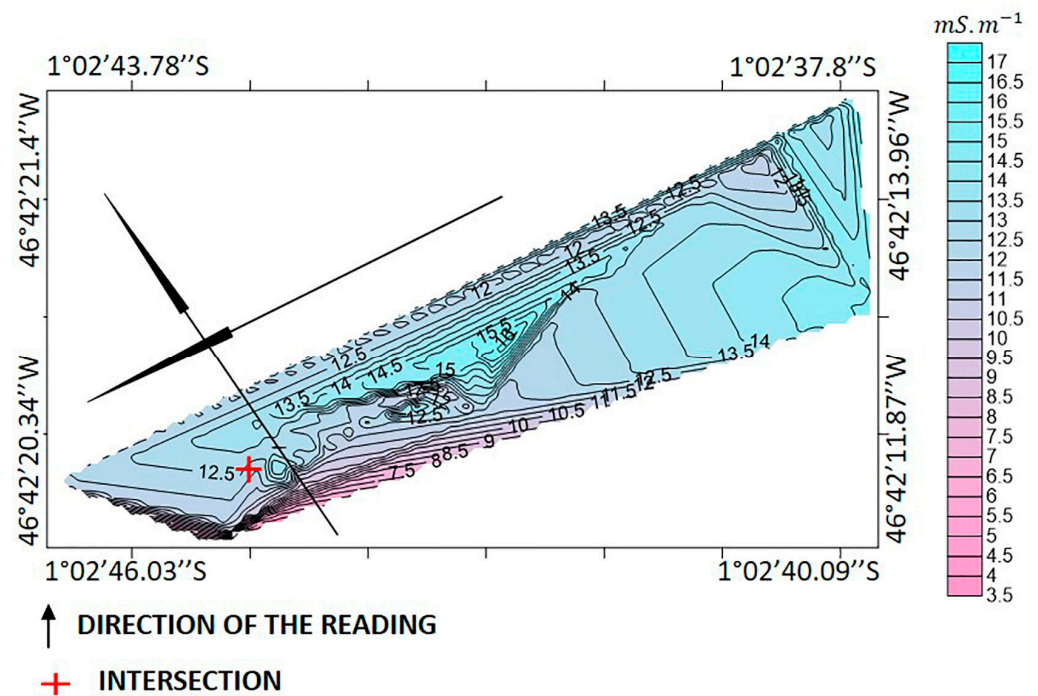


Figure 6. Map of the apparent conductivity recorded in Area 1 (Bragança), with a Horizontal Dipole (HD) and antennas with a 10 m interval between coils.

In Area 1 (Bragança) organic matter was identified, which was derived from the decomposition of vegetation at the site. The sedimentological analysis of the soil detected the presence of three layers, one of clay (top), then silt, and finally sand (bottom). The soil is clayey, with a 40–60% clay content.

Three Standard Penetration Test (SPT) probes—SP 01 (01°02.685' S, 46°42.231' W), SP 02 (01°02.679' S, 46°42.228' W), and SP 03 (01°02.669' S, 46°42.240' W)—were implemented in study Area 1 (Figure 3b). The depth limits of these probes were between 10.45 m (SP 01, SP 02) and 10.50 m (SP 03). The lithological profiles for each SPT probe are shown in Tables 1 and 2.

Table 1. Lithological profile of the subsoil obtained by SPT probes SP 01 and SP 02, which was implemented in study Area 1 (CEANPA, Bragança) [60].

Depth (m)	SPT Probes SP 01 and SP 02
0–4.769	Sandy silt, yellow
4.77–9.299	Medium clay with pebbles
9.30–10.45	Coarse sand, reddish and yellow

Table 2. Lithological profile of the subsoil obtained by SPT probe SP 03, which was implemented in study Area 1 (CEANPA, Bragança) [60].

Depth (m)	SPT Probe SP 03
0–4.769	Sandy silt, yellow
4.77–9.299	Medium clay with pebbles
9.30–10.50	Coarse sand, reddish and yellow

Probes SP 01 and SP 02 identified three layers, containing sandy silt, clay with pebbles, and coarse sand (Table 1). Similar lithological layers were identified by probe SP 03 (Table 2).

The AB profile (Figure 5a) was also used to calculate the propagation velocity and the relative dielectric permittivity (dielectric constant), which were used to determine the

lithology of the different layers of the subsoil in Area 1 (Table 3). The values obtained for these parameters revealed a lithological profile that aligned closely with the findings of the SPT probes in the same area.

Table 3. Dielectric permittivity (ϵ) and electromagnetic wave velocity (v) measured from the different layers of the subsoil in study Area 1 (CEANPA, Bragança).

Depth (m)	Lithology [60]	Wave Velocity (m/ns)	Dielectric Permittivity (ϵ_r)
0–4.769	Sandy silt, yellow	0.092	10.63
4.77–8.5	Medium clay with pebbles	0.070	18.37

3.2. Area 2

The 200 and 400 MHz antennas were also used in Area 2 (Tracuateua), where the GPR prospection reached a depth of 7.5–8.5 m but, once again, with high noise levels at depths of below 1 m (Figure 7). Horizontal layers were identified near the surface, between 0 and 1 m (AB profile, Figure 7a). In this profile, a horizontal reflector was also identified at 6–6.5 m, which corresponds to the local water table, as confirmed by a well drilled on the property, in which brackish water was found at a depth of 6.0 m.

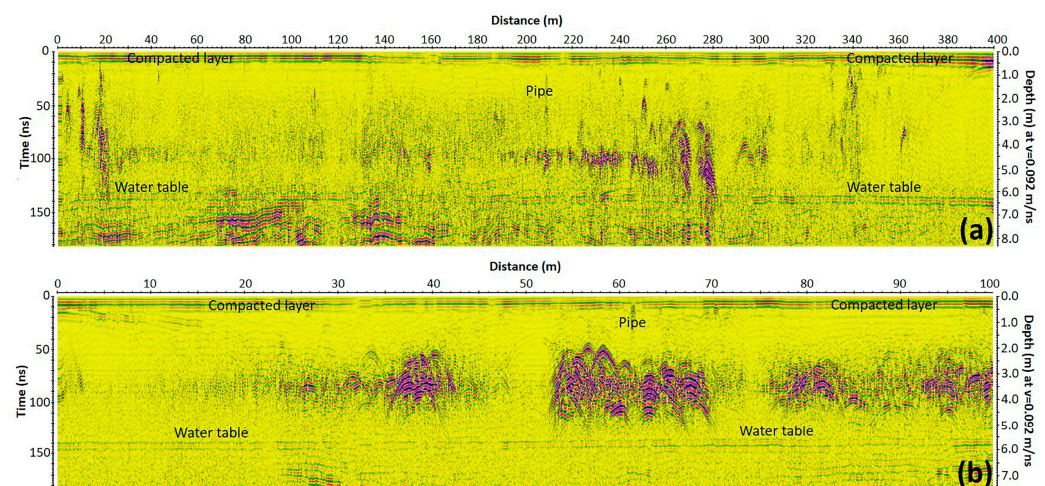


Figure 7. The GPR profiles (200 MHz antenna with a 200 ns time window) recorded in Area 2 (Tracuateua): (a) AB; (b) CD.

The CD profile (Figure 7b) had a number of features that were similar to those of the AB profile (Figure 7a), including horizontal layers (0–1 m) and a water table at 5.5–6 m, as well as hyperbole-shaped reflectors at depths of between 1.75 m and 5 m, which would appear to indicate the presence of buried pipes.

These profiles (Figure 7) are color-coded as in those of Figure 5, where the yellow shading indicates a zone of low amplitude due to the attenuation of the GPR signal. The other colors represent zones of high amplitude or reflection.

The conductivity was higher in Area 1, with values ranging from 16 to 48 $\text{mS}\cdot\text{m}^{-1}$ (Figure 8). These values are also consistent with the presence of a clayey subsoil [38]. These soils are of the yellow latosol type [65].

The soil samples collected from Area 2 (Tracuateua) have a very high clay fraction (60–100%), in particular, at depths of below 1 m. The occurrence of organic matter was very similar to that observed in Area 1.

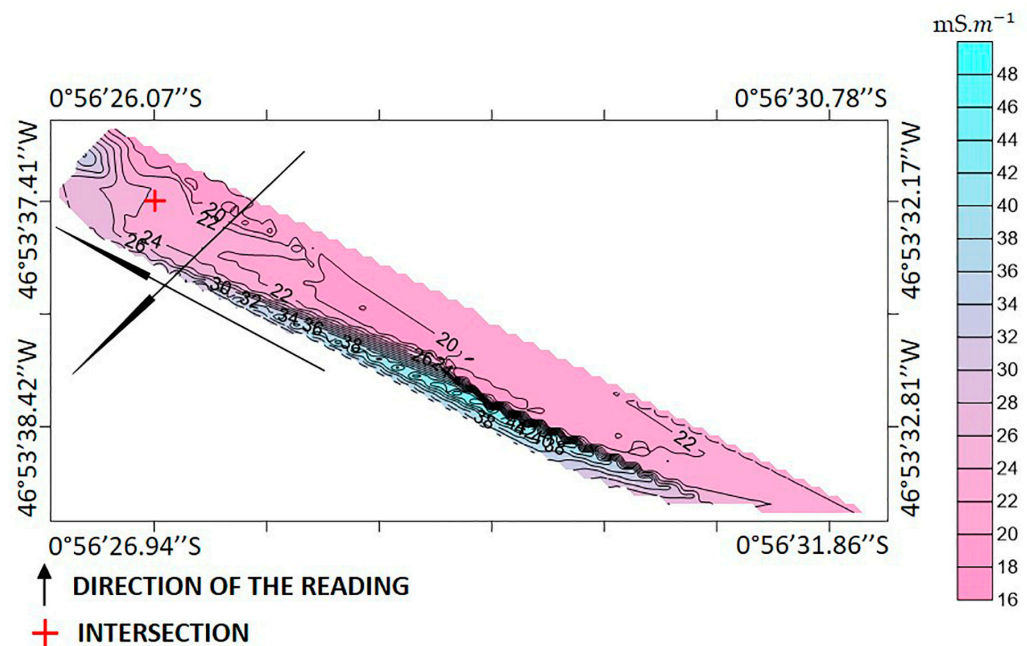


Figure 8. Map of the apparent conductivity recorded in Area 2 (Tracuateua), with a Horizontal Dipole (HD) and antennas with a 10m interval between coils.

4. Discussion

In the present study, the soils were humid due to the effects of the local rainy season. The saturation of soils with water increases their electrical conductivity and attenuates the GPR signal. In general, the electrical conductivity of a soil is determined by its content of different types of clay minerals [66]. Low-frequency (<200 MHz) antennas provide a lower resolution and a greater penetration depth, while higher frequency (>200 MHz) antennas obtain a higher resolution [29].

However, the penetration of the GPR signal into the terrain will depend on its conductivity and resistivity, irrespective of the frequency of the antenna used. In environments with low conductivity (or high resistivity), such as dry, sandy soils, the radar signal may reach depths of over 15 m, whereas in conductive environments, such as saturated clay soils, the radar signal may be reduced to depths of less than 1 m [29].

The GPR technique has been used to provide a reliable interpretation of features such as near-surface structures, hydrological processes, and the depth of the water table (e.g., [67–73]). Reference [74] used GPR to evaluate the conditions of a terrain earmarked for aquaculture in the Montenegro zone of Bragança (Pará, Brazil). These authors identified a sequence of normal faults with minor slips, a depression (35m in length at a depth of 2.8 m), and reflectors in the form of hyperboles of energy dispersal, which were assumed to represent the pipes used to install the fish ponds. The amplitude of the electromagnetic signal also varied considerably, with the GPR signature of the local rocky substrate, formed by parallel and subparallel reflectors with a low reflection zone. A horizontal reflector was identified at a depth of 4.48–4.62 m, which corresponds to the top of the water table, according to the depth of the wells drilled at the site.

The authors of a number of previous studies have considered the electrical conductivity as an important parameter for the evaluation of the quality of terrains earmarked for aquaculture (e.g., [4,75,76]). Reference [4] analyzed several parameters of soil samples of fish ponds of different ages (1–5 years and >5 years) in Noakhali, Bangladesh. The electrical conductivity of the new ponds (334.8 mS.m^{-1}) was much higher than that of the older ponds (130.6 mS.m^{-1}).

In a study of soil samples from the pond at Circuit House in Balochistan, Pakistan, [77] recorded electrical conductivity of no more than 290 mS.m^{-1} , which was still considered to be favorable for aquaculture, although an overall mean value of $221 \pm 143 \text{ mS.m}^{-1}$ was

recorded in this study. Reference [75] evaluated the conditions of terrains earmarked for aquaculture in the divisions of Lahore, Gujranwala, Sahiwal, and Sargodha, in the Punjab district of Pakistan. The results of the surveys (electrical conductivity, soil particle size, pH, and salinity) indicated the presence of soils that were suitable for the construction of fish ponds at most of the sites in Lahore, Sargodha, and Sahiwal.

In addition to the available geophysical tools, which have their own physical properties, a number of other potential methods based on geotechnology are available [11], which have been integrated with other approaches (e.g., the AHP, ANP, and MCDM methods), to identify the sites most appropriate for inland aquaculture [12,20,21,78–82]. An integrated approach of this type was applied to select sites for fish farming in M'diq Bay in Morocco [6]. This study applied an integrated approach that involved the GIS-Spatial Multi-Criteria Evaluation (SMCE) and Analytical Hierarchy Process (AHP) methods and the Weighted Linear Combination (WLC) approach to select polygons suitable for fish farming, together with the carrying capacity approach to define the most suitable number of fish farms.

The Multi-Criteria Evaluation (MCE) method was employed to optimize the selection of sites appropriate for sturgeon farming on the southern coast of the Caspian Sea, in Golestan, Iran. In this approach, the MCE was weighted using the Analytic Hierarchy Process (AHP) and combined with the Weighted Linear Combination (WLC) approach [83]. Reference [84] also applied this method to the survey of areas for the development of shellfish farming in Souahlia Bay, in Algeria.

A multi-criteria approach was used to identify sites that were adequate for fresh- and brackish water fish farming on the coastal plains of the Indian states of Odisha and Tamil Nadu. For this, they used large scale (1:10,000), high resolution maps of land cover and use, with thematic layering and regulations [85]. Reference [86] successfully applied a combined approach of Earth Observation (EO) and a dynamic energy budget (DEB) model for the selection of the most appropriate sites for the cultivation of the Pacific oyster, *Crassostrea gigas*, on the coast of South Africa.

The sedimentological analyses carried out in the present study provided confirmation of the geophysical methods employed at the different study sites. The results of the SPT technique (Tables 1 and 2) validated the findings of the EMI and GPR tools (Table 3) on the lithological characteristics of the subsoil (Area 1). The relative dielectric constants and electromagnetic wave velocities of the geological substrates were determined as in Area 1 [38]. The lithological features identified in Area 1 were also corroborated using the Brazilian Geological Service (BGS) database on the subterranean waters of the study area [87], which correspond to the Barreiras Formation of the Neogene, in Area 1, formed by interlaced sandy-clayey and clay soils with medium to coarse sands, and the Quaternary in Area 2, with the intercalation of clayey and sandy-clayey soils, containing medium-grained sand.

The sedimentological analysis of the soil samples confirmed that the substrates at the two study sites are appropriate for the construction of fish ponds, based on the recommendations of [57,58]. The results of these analyses were also consistent with the results of the EM and GPR surveys.

The present study confirmed the good performance of the geophysical tools for the diagnosis of terrains earmarked for fish farming. These tools identified favorable conditions in the subsurface at CEANPA (Area 1). These results supported the excavation of fifteen ponds (twelve for raising fish, two for the treatment of wastewater, and one reservoir) at this site in February 2020 (Figure 9), although this process was interrupted due to the COVID-19 pandemic and was only completed in December 2021 (Figure 3b). The initial excavations confirmed the findings of the geophysical survey and the sedimentological analyses. The maximum depth of these ponds is approximately 1.6 m (Figure 10).



Figure 9. Aquaculture operations in Area 1: (a) Installations; (b) Demarcation of the ponds; (c–f) Excavated ponds.



Figure 10. The maximum depth of the ponds excavated in Area 1.

Ground Penetrating Radar (GPR) and Electromagnetic Induction (EMI) can be extremely valuable for the collection of spatial data that correlate with the soil types and hydrological properties of a terrain (e.g., [88–92]). The geophysical survey techniques employed in the present study have also been used to successfully investigate the physical properties of the soil and subsoil in research in scientific fields such as agronomy,

archeology, hydrology, and wetland ecology (e.g., [23,37,88,93–106]). References [22,107] predicted that the integration of geophysical tools (e.g., Electrical Resistivity Tomography (ERT), EMI, and GPR) with remote sensing will contribute to the successful development of precision agriculture.

5. Conclusions

The radargrams identified a depression in Area 1 (Bragança), which appears to have been filled with material at some time in the past. A compacted layer was also detected near the surface, although no evidence of a water table was found at this site.

In Area 2 (Tracuateua), the GPR prospection identified a horizontal reflector (6–6.5 m) corresponding to the water table, which was confirmed by a well drilled on the property. Two other features recorded at this site were a stack of horizontal layers approximately 1 m thick and hyperbole-shaped reflectors that may represent the presence of buried pipes.

The EMI survey identified the soils in both study areas, at depths of up to 7.5 m. The characteristics of the soils of both areas were found to be appropriate for fish farming. In Area 1, the Horizontal Dipole (HD) with the antennas at 10 m intervals recorded low levels of conductivity, between 3.5 and 17 $\text{mS}\cdot\text{m}^{-1}$, which indicate the presence of a clayey subsoil. In Area 2, conductivity was between 16 and 48 $\text{mS}\cdot\text{m}^{-1}$, which also indicates the presence of a clayey substrate.

The preliminary sedimentological analyses identified clayey soils (23–60% clay) in Area 1 and very clayey soils (60–100% clay) in Area 2, which confirmed the lithology of the subsoil identified using the EM34-3 electrical conductivity meter.

The dielectric characteristics and the propagation velocities of the electromagnetic (EM) wave determined the lithology of the principal strata of Area 1, which were validated by the SPT probes.

The combined (GPR + EMI) geophysical approach permitted the acquisition of valid, complementary data on the subsurface that provide reliable information on the characteristics of the soils of the study areas earmarked for the installation of aquaculture projects.

Based on these findings, we would recommend the integrated application of GPR and EM34-3 tools, combined with sedimentological analyses and the SPT, for the diagnosis of the characteristics of the subsoil of areas earmarked for aquaculture projects. This approach will guarantee the data needed to evaluate the configuration of the subsoil, which may be fundamental to ensure an adequate decision-making process during the development of aquaculture projects, by both minimizing the environmental impacts and guaranteeing the maximum economic returns of the operation. This type of approach can also be applied to the evaluation of the sites of small dams, tailing pits, mud pits, water holding installations, and even wildlife refuges. In the case of deeper geology, however, the use of Electrical Resistivity Tomography (ERT) is recommendable. Even so, a more detailed analysis would require the complementary use of lower-frequency GPR.

Ground Penetrating Radar can also be used to obtain bathymetric data and bottom stratigraphic sediment profiles from natural freshwater environments, such as rivers and lakes. This freshwater GPR technique cannot be used in salt or brackish water environments.

Future studies may benefit from the use of high dynamic range GPR with a built-in GPS and integrated odometer, to minimize spatial distortions during data collection, which ensures the quality of the data for processing.

Author Contributions: Conceptualization, R.W.T.P., P.A.C.O., and F.A.A.; Methodology, R.W.T.P. and P.A.C.O.; Validation, R.W.T.P., P.A.C.O., and F.A.A.; Formal Analysis, R.W.T.P., P.A.C.O., and F.A.A.; Investigation, R.W.T.P. and P.A.C.O.; Resources, R.W.T.P. and P.A.C.O.; Data Curation, R.W.T.P. and P.A.C.O.; Writing—preparation of original draft, P.A.C.O. and F.A.A.; Writing—Review and Editing, P.A.C.O. and F.A.A.; Supervision, P.A.C.O. and F.A.A.; Project Administration, P.A.C.O. All authors have read and agreed to the published version of the manuscript.

Funding: Dean of Research and Graduate Studies-PROPESP/Federal University of Pará-UFGA (Brazil). F.A.A. is a CNPq (Conselho Nacional de Desenvolvimento Científico e Tecnológico, Brazil) research fellow.

Institutional Review Board Statement: Not applicable.

Informed Consent Statement: Not applicable.

Data Availability Statement: The data in this study are available on request from the corresponding author.

Acknowledgments: We would like to thank the Federal University of Pará at the Bragança campus for allowing us to conduct the surveys at the future CEANPA aquaculture research center (Area 1) and the Gomes family for giving us permission to conduct the surveys on their property (Area 2). We would also like to thank the reviewers for their valuable comments that helped to improve the manuscript substantially. We would like to thank Zélia Pimentel Nunes for the photos provided for Figure 9. Finally, we would also like to thank the Faculty of Geophysics (Institute of Geosciences (IG)/UFGA, Belém, Brazil) for the providing the EM34-3 instrument.

Conflicts of Interest: The authors declare no conflict of interest.

References

1. Calixto, E.S.; dos Santos, D.F.B.; Lange, D.; Galdiano, M.S.; Rahman, I.U. Aquaculture in Brazil and worldwide: Overview and perspectives. *J. Environ. Anal. Prog.* **2020**, *5*, 98–107. [CrossRef]
2. MAPA (Ministério da Agricultura, Pecuária e Abastecimento). *Plano Nacional de desenvolvimento da aquicultura—PNDA*; Departamento de Ordenamento e Desenvolvimento da Aquicultura: Brasília, Brazil, 2017. Available online: https://www.gov.br/agricultura/pt-br/assuntos/mpa/aquicultura-1/plano-nacional-de-desenvolvimento-da-aquicultura-pnda-2022-2032/documento-pnda-30122022-1-_m.pdf (accessed on 21 September 2023). (In Portuguese)
3. Aheto, D.W.; Acheampong, E.; Odoi, J.O. Are small-scale freshwater aquaculture farms in coastal areas of Ghana economically profitable? *Aquac. Int.* **2019**, *27*, 785–805. [CrossRef]
4. Tapader, M.A.; Hasan, M.M.; Sarker, B.S.; Rana, E.U.; Bhowmik, S. Comparison of soil nutrients, pH and electrical conductivity among fish ponds of different ages in Noakhali, Bangladesh. *Korean J. Agric. Sci.* **2017**, *44*, 16–22. [CrossRef]
5. FAO (Food and Agriculture Organization of the United Nations). *The State of World Fisheries and Aquaculture 2022. Towards Blue Transformation*; FAO: Rome, Italy, 2022. [CrossRef]
6. Nhhala, I.; Bahida, A.; Nhhala, H.; Chadli, H.; Baldan, D.; Wahbi, M.; Erraioui, H. Site selection for fish farming using integrated GIS-spatial multi-criteria evaluation and carrying capacity approaches: Case study of M'diq bay, Morocco. *Egypt. J. Aquat. Biol. Fish.* **2022**, *26*, 807–841. [CrossRef]
7. Tian, P.; Liu, Y.; Li, J.; Pu, R.; Cao, L.; Zhang, H.; Ai, S.; Yang, Y. Mapping Coastal Aquaculture Ponds of China Using Sentinel SAR Images in 2020 and Google Earth Engine. *Remote Sens.* **2022**, *14*, 5372. [CrossRef]
8. EMBRAPA (Empresa Brasileira de Pesquisa Agropecuária). *Piscicultura de água Doce: Multiplicando Conhecimentos*; EMBRAPA: Brasília, Brazil, 2013; 440p, Available online: <https://www.infoteca.cnptia.embrapa.br/handle/doc/1082280> (accessed on 29 August 2023). (In Portuguese)
9. SEBRAE (Serviço Brasileiro de Apoio às Micro e Pequenas Empresas). *Como Iniciar Piscicultura Com Espécies Regionais*, 1st ed.; SEBRAE: Brasília, Brazil, 2013; Available online: [https://bibliotecas.sebrae.com.br/chronus/ARQUIVOS_CHRONUS/bds/bds.nsf/b7c92dacee0fbaec6c77bbb438c6ab64/\\$File/4510.pdf](https://bibliotecas.sebrae.com.br/chronus/ARQUIVOS_CHRONUS/bds/bds.nsf/b7c92dacee0fbaec6c77bbb438c6ab64/$File/4510.pdf) (accessed on 21 September 2023). (In Portuguese)
10. Jayanthi, M.; Thirumurthy, S.; Samynathan, M.; Manimaran, K.; Duraisamy, M.; Muralidhar, M. Assessment of land and water ecosystems capability to support aquaculture expansion in climate-vulnerable regions using analytical hierarchy process based geospatial analysis. *J. Environ. Manag.* **2020**, *270*, 110952. [CrossRef]
11. SENAR (Serviço Nacional de Aprendizagem Rural). *Aquicultura: Planejamento e Legalização de Projetos Aquícolas*, 2nd ed.; SENAR: Brasília, Brazil, 2018; 84p. (In Portuguese)
12. Hadipour, A.; Vafaie, F.; Hadipour, V. Land suitability evaluation for brackish water aquaculture development in coastal area of Hormozgan, Iran. *Aquac. Int.* **2014**, *23*, 329–343. [CrossRef]
13. GESAMP (IMO/FAO/UNESCO-IOC/WMO/WHO/IAEA/UN/UNEP). Joint group of experts on the scientific aspects of marine environmental Protection. Planning and management for sustainable coastal aquaculture development. *FAO Rep. Stud.* **2001**, *68*, 90.
14. SEBRAE (Serviço Brasileiro de Apoio às Micro e Pequenas Empresas). *Aquicultura: Um mercado em crescimento no Brasil e no mundo*. 2022. Available online: <https://sebrae.com.br/sites/PortalSebrae/artigos/aquicultura-um-mercado-em-crescimento-no-brasil-e-no-mundo,ac99bb738c910810VgnVCM100000d701210aRCRD> (accessed on 21 September 2023). (In Portuguese)
15. PEIXE BR. Associação Brasileira de Piscicultura. *Anuário PEIXE BR da Piscicultura 2023*. São Paulo (SP). Brazil. 2023. Available online: <https://www.peixebr.com.br/anuario/> (accessed on 21 September 2023). (In Portuguese)

16. Valenti, W.C.; Barros, H.P.; Moraes-Valenti, P.; Bueno, G.W.; Cavalli, R.O. Aquaculture in Brazil: Past, present and future. *Aquac. Rep.* **2021**, *19*, 100611. [[CrossRef](#)]
17. Krause, G.; Stead, S.M. Governance and offshore aquaculture in multi-resource use settings. In *Aquaculture Perspective of Multi-Use Sites in the Open Ocean*; Buck, B.H., Langan, R., Eds.; Springer: Cham, Switzerland, 2017; pp. 149–162. [[CrossRef](#)]
18. Dapieve, D.R.; Maggi, M.F.; Mercante, E.; Francisco, H.R.; Oliveira, D.D.D.; Luiz Junior, O.J. Use of geotechnologies for aquaculture site selection: Suitability factors and constraints for production in ground-excavated ponds. *Lat. Am. J. Aquat. Res.* **2023**, *5*, 160–194. [[CrossRef](#)]
19. Falconer, L.; Middelboe, A.L.; Kaas, H.; Ross, L.G.; Telfer, T.C. Use of geographic information systems for aquaculture and recommendations for the development of spatial tools. *Rev. Aquacult.* **2019**, *12*, 664–677. [[CrossRef](#)]
20. Snyder, J.; Boss, E.; Weatherbee, R.; Thomas, A.C.; Brady, D.; Newell, C. Oyster Aquaculture Site Selection using Landsat 8-Derived Sea Surface Temperature, Turbidity, and Chlorophyll a. *Front. Mar. Sci.* **2017**, *4*, 190. [[CrossRef](#)]
21. Jiang, B.; Boss, E.; Kiffney, T.; Hesketh, G.; Bourdin, G.; Fan, D.; Brady, D.C. Oyster Aquaculture Site Selection Using High-Resolution Remote Sensing: A Case Study in the Gulf of Maine, United States. *Front. Mar. Sci.* **2022**, *9*, 802438. [[CrossRef](#)]
22. Pradipta, A.; Soupios, P.; Kourgialas, N.; Doula, M.; Dokou, Z.; Makkawi, M.; Alfarhan, M.; Tawabini, B.; Kirmizakis, P.; Yassin, M. Remote Sensing, Geophysics, and Modeling to Support Precision Agriculture—Part 1: Soil Applications. *Water* **2022**, *14*, 1158. [[CrossRef](#)]
23. Bitella, G.; Rossi, R.; Loperte, A.; Satriani, A.; Lapenna, V.; Perniola, M.; Amato, M. Geophysical Techniques for Plant, Soil, and Root Research Related to Sustainability. In *The Sustainability of Agro-Food and Natural Resource Systems in the Mediterranean Basin*; Vastola, A., Ed.; Springer International Publishing AG: Cham, Switzerland, 2015; 397p.
24. Besson, A.; Cousin, I.; Bourennane, H.; Nicoullaud, B.; Pasquier, C.; Richard, G.; Dorigny, A.; King, D. The spatial and temporal organization of soil water at the field scale as described by electrical resistivity measurements. *Eur. J. Soil Sci.* **2010**, *61*, 120–132. [[CrossRef](#)]
25. Gomes, K.J.M.; Oliva, P.A.C.; da Rocha, H.O.; Mendes, R.d.A.; da Costa, A.C.G.; Miranda, C.d.S.; Almeida, N.d.O. Evaluation of the contamination of the subsurface and groundwater by monoaromatic hydrocarbons in an eastern Amazonian town in northern Brazil. *Environ. Earth Sci.* **2023**, *82*, 23. [[CrossRef](#)]
26. Delgado, L.F.S.; Oliva, P.A.C.; El Robrini, M.; dos Reis Junior, J.A. Contribution of ground penetrating radar in the study of an Amazon tide channel, influenced by macro tide. *J. S. Am. Earth Sci.* **2022**, *116*, 103776. [[CrossRef](#)]
27. Bacha, D.d.C.S.; Santos, S.; Mendes, R.d.A.; Rocha, C.C.d.S.; Corrêa, J.A.; Cruz, J.C.R.; Abrunhosa, F.A.; Oliva, P.A.C. Evaluation of the contamination of the soil and water of an open dump in the Amazon Region, Brazil. *Environ. Earth Sci.* **2021**, *80*, 113. [[CrossRef](#)]
28. Sousa, C.N.d.C., Jr.; El Robrini, M.; Oliva, P.A.C. Experimental survey of the Ground Penetrating Radar (GPR) in the study of the Aturiaí river (Bragança Coastal Plain, northeast of Pará). *Res. Soc. Dev.* **2020**, *9*, 1–29. [[CrossRef](#)]
29. de Souza, L.A.P.; Gandolfo, O.C.B. Geofísica aplicada. In *Geologia de Engenharia e Ambiental: Métodos e técnicas*, 1st ed.; Oliveira, A.M.S., Monticeli, J.J., Eds.; ABGE—Associação Brasileira de Geologia de Engenharia and Ambiental: São Paulo, Brazil, 2018; Volume 2, pp. 314–333.
30. Utsi, E.C. *Ground Penetrating—Radar Theory and Practice*. Butterworth-Heinemann; Elsevier Ltd.: Amsterdam, The Netherlands, 2017.
31. Haynie, K.L.; Khan, S.D. Shallow subsurface detection of buried weathered hydrocarbons using GPR and EMI. *Mar. Pet. Geol.* **2016**, *77*, 116–123. [[CrossRef](#)]
32. Kaya, M.A.; Özürlan, G.; Şengül, E. Delineation of soil and groundwater contamination using geophysical methods at a waste disposal site in Çanakkale, Turkey. *Environ. Monit. Assess.* **2007**, *135*, 441–444. [[CrossRef](#)] [[PubMed](#)]
33. Chira, O.P.; Barbalho, D.P.; Cruz, J.C.R. Environmental study of the Bragança City landfill (Brazil) applying Ground Penetrating Radar. In Proceedings of the 21st European Meeting of Environmental and Engineering Geophysics (EAGE 2015), Turin, Italy, 6–10 September 2015. [[CrossRef](#)]
34. Rosales, R.M.; Martínez-Pagan, P.; Faz, A.; Moreno-Cornejo, J. Environmental Monitoring Using Electrical Resistivity Tomography (ERT) in the Subsoil of Three Former Petrol Stations in SE of Spain. *Water Air Soil Pollut.* **2012**, *223*, 3757–3773. [[CrossRef](#)]
35. Jol, H.M. (Ed.) *Ground Penetrating Radar: Theory and Applications*; Elsevier Science: Amsterdam, The Netherlands, 2009. [[CrossRef](#)]
36. Kaya, M.A.; Özürlan, G.; Balkaya, Ç. Geoelectrical investigation of seawater intrusion in the coastal urban area of Çanakkale, NW Turkey. *Environ. Earth Sci.* **2015**, *73*, 1151–1160. [[CrossRef](#)]
37. Kearey, P.; Brooks, M.; Hill, I. *An Introduction to Geophysical Exploration*; Blackwell Science Ltd.: London, UK, 2002.
38. Davis, J.L.; Annan, A.P. Ground-penetrating radar for high-resolution mapping of soil and rock stratigraphy. *Geophys. Prospect.* **1989**, *37*, 531–551. [[CrossRef](#)]
39. Doolittle, J.A.; Brevik, E.C. The use of electromagnetic induction techniques in soils studies. *Geoderma* **2014**, *223–225*, 33–45. [[CrossRef](#)]
40. Emmanuel, E.D.; Doro, K.O.; Iserhien-Emekeme, R.E.; Atakpo, E.A. Using geophysics to guide the selection of suitable sites for establishing sustainable earthen fishponds in the Niger-Delta region of Nigeria. *Heliyon* **2023**, *9*, e17618. [[CrossRef](#)]
41. Chira, P.A.; Teixeira, F.d.A.d.S.; Pena, R.T.; dos Reis Júnior, J.A. Application of the Ground Penetrating Radar (GPR) and sedimentology for evaluation of the subsoil for the excavation of fish farming ponds in the municipality of Bragança, Northeastern Pará, Brazil. In Proceedings of the 17o Simpósio de Geologia da Amazônia. Geotecnologias e Sustentabilidade: A Geologia na Amazônia atual, Santarém, Pará, Brazil, 23–25 October 2023.

42. Pathirana, S.; Lambot, S.; Krishnapillai, M.; Cheema, M.; Smeaton, C.; Galagedara, L. Ground-Penetrating Radar and Electromagnetic Induction: Challenges and Opportunities in Agriculture. *Remote Sens.* **2023**, *15*, 2932. [CrossRef]
43. IBGE (Instituto Brasileiro de Geografia e Estatística). Divisão Regional do Brasil em Regiões Geográficas Imediatas e regiões Geográficas Intermediárias. Rio de Janeiro. 2017. Available online: <https://biblioteca.ibge.gov.br/index.php/biblioteca-atálogo?view=detalhes&id=2100600> (accessed on 5 September 2022). (In Portuguese)
44. Aranha, L.G.; Lima, H.P.; Souza, J.M.P.; Marinho, R.K. Origem and evolução das bacias de Bragança-Viseu, São Luís and Ilha Nova. In *Origem and Evolução de Bacias Sedimentares*; Raja Gabaglia, G.P., Milani, E.J., Eds.; Petrobrás: Rio de Janeiro, Brazil, 1990; pp. 221–233. (In Portuguese)
45. Costa, J.B.S.; Hasui, Y. Evolução geológica da Amazônia. In *Contribuições a Geologia da Amazônia*; Costa, M.L., Angélica, R.S., Eds.; Brazilian Society of Geology/FINEP: Belém, Brazil, 1997; pp. 15–90. (In Portuguese)
46. Costa, J.B.S.; Borges, M.S.; Bermeguy, R.L.; Fernandes, J.M.G.; Costa Júnior, P.S.; Costa, M.L. Evolução cenozóica da região de Salinópolis, nordeste do estado do Pará. *Geociências* **1993**, *12*, 353–372. (In Portuguese)
47. Igreja, H.L.S. Aspectos tectono-sedimentares do Fanerozóico do nordeste do Pará e nordeste do Maranhão. Ph.D. Thesis, Federal University of Pará, Belem, Brazil, 1991.
48. de Moraes, B.C.; da Costa, J.M.N.; da Costa, A.C.L.; Costa, M.H. Variação espacial e temporal da precipitação no estado do Pará. *Acta Amaz.* **2005**, *35*, 207–214. (In Portuguese) [CrossRef]
49. Magalhães, A.; Costa, R.M.; Liang, T.H.; Pereira, L.C.C.; Ribeiro, M.J.S. Spatial and temporal distribution in density and biomass of two Pseudodiaptomus species (Copepoda: Calanoida) in the Caeté River Estuary (Amazon region-North of Brazil). *Braz. J. Biol.* **2006**, *66*, 421–430. [CrossRef]
50. Annan, A.P. Electromagnetic principles of Ground Penetrating Radar. In *Ground Penetrating Radar—Theory and Applications*; Jol, H.M., Ed.; Elsevier: Amsterdam, The Netherlands, 2009; pp. 3–40.
51. McNeill, J.D. *Electromagnetic Terrain Conductivity at Low Induction Numbers*; Technical Note TN-6; Geonics Limited: Mississauga, ON, Canada, 1980; pp. 1–15.
52. Kuang, B.; Mahmood, H.S.; Quraishi, M.Z.; Hoogmoed, W.B.; Mouazen, A.M.; Van Henten, E.J. Sensing Soil Properties in the Laboratory, In Situ, and On-Line: A Review. *Adv. Agron.* **2012**, *114*, 155–224. [CrossRef]
53. Moreira, C.A.; Aquino, W.F.; Dourado, J.C. Aplicação do método eletromagnético indutivo (EM) no monitoramento de contaminantes em subsuperfície. *Rev. Bras. Geofísica* **2007**, *25*, 413–420. (In Portuguese) [CrossRef]
54. Associação Brasileira de Normas Técnicas (ABNT). Norma Brasileira NBR 6484. *Solo-Sondagens de Simples reconhecimento com SPT—Método de Ensaio*. 2001. Available online: https://engenhariacivilfsp.files.wordpress.com/2014/11/spt-metodo_de_ensaio_nbr_6484.pdf (accessed on 16 August 2022). (In Portuguese)
55. GEOSCAN. GEOSCAN Geology and Geophysics Cia. *Standard Penetration Test (SPT): Know All the Procedures*. 2022. Available online: <https://www.geoscan.com.br/blog/spt/> (accessed on 16 August 2022). (In Portuguese)
56. Google Earth Pro 2021. Available online: <https://www.google.com/earth/versions/> (accessed on 13 June 2021).
57. Basudha, C.h.; Singh, R.K.; Sureshchandra, N.; Soranganba, N.; Sobita, N.; Singh, T.B.; Singh, L.K.; Singh, I.M.; Prakash, N. *Fish Farm Design and Pond Construction for Small Scale Fish Farming in Manipur*; Technical Bulletin No. RCM(TB)-12, ICAR Research Complex for NEH Region; Manipur Centre: Imphal, India, 2019; pp. 3–4.
58. Boyd, C.E. *Bottom Soils, Sediment, and Pond Aquaculture*; Springer Science + Business Media Dordrecht: Dordrecht, The Netherlands, 1995.
59. Neto, J.C.P.; Costa, J.d.O. *Análise do Solo: Determinações, Cálculos and Interpretação*; Empresa de Pesquisa Agropecuária de Minas Gerais (EPAMIG Sul de Minas): Lavras, Brazil, 2012; pp. 1–14. Available online: http://www.bibliotecaflorestal.ufv.br/bitstream/handle/123456789/10529/EPAMIG_An%c3%a1lise-do-solo-determina%c3%a7%c3%b5es-c%c3%a1culos-e-interpreta%c3%a7%c3%a3o.pdf?sequence=1&isAllowed=y (accessed on 14 May 2020).
60. PLENO. Pleno Arquitetura E Construções. Geotechnical Survey Report requested by the Federal University of Pará (Brazil) for the Northeast Pará Aquaculture Research Center (CEANPA). 2015. (In Portuguese)
61. da Rocha, H.O.; Silva, M.W.C.; Marques, F.L.T.; Leite Filho, D.C. Magnetic gradiometry and ground penetrating radar applied in Estearia of Penalva (MA). *Geol. USP Sér. Cient.* **2015**, *15*, 3–14. [CrossRef]
62. Reis, A.R., Jr.; Castro, D.L.; Jesus, T.E.S.; Lima Filho, F.P. Characterization of collapsed paleocave systems using GPR attributes. *J. Appl. Geophys.* **2014**, *103*, 43–56. [CrossRef]
63. Yelf, R. Where is True Time Zero? In Proceedings of the Tenth International Conference on Grounds Penetrating Radar, Delft, The Netherlands, 21–24 June 2004; pp. 279–282.
64. Annan, A.P. Transmission dispersion and GPR. *J. Environ. Eng. Geophys.* **1996**, *2*, 125–136. [CrossRef]
65. EMBRAPA (Empresa Brasileira de Pesquisa Agropecuária). *Recomendações de calagem e adubação para o estado do Pará*, 2nd ed.; Brasil, E.C., Cravo, M.d.S., Viégas, I.d.J.M., Eds.; EMBRAPA: Brasília, Brazil, 2020; 424p. (In Portuguese)
66. McNeill, J.D. *Electrical Conductivity of Soils and Rock*; Technical Note TN-5; Geonics Limited: Mississauga, ON, Canada, 1980.
67. Sonkamble, S.; Chandra, S. GPR for earth and environmental applications: Case studies from India. *J. Appl. Geophys.* **2021**, *193*, 104422. [CrossRef]
68. Paz, C.; Alcalá, F.J.; Carvalho, J.M.; Ribeiro, L. Current uses of ground penetrating radar in groundwater-dependent ecosystems research. *Sci. Total Environ.* **2017**, *595*, 868–885. [CrossRef]

69. Zhang, J.; Lin, H.; Doolittle, J. Soil layering and preferential flow impacts on seasonal changes of GPR signals in two contrasting soils. *Geoderma* **2014**, *213*, 560–569. [CrossRef]
70. Nováková, E.; Karous, M.; Zajíček, A.; Karousová, M. Evaluation of ground penetrating radar and vertical electrical sounding methods to determine soil horizons and bedrock at the locality Dehtáře. *Soil Water Res.* **2013**, *8*, 105–112. [CrossRef]
71. Doetsch, J.; Linde, N.; Pessognelli, M.; Green, A.G.; Günther, T. Constraining 3-D electrical resistance tomography with GPR reflection data for improved aquifer characterization. *J. Appl. Geophys.* **2012**, *78*, 68–76. [CrossRef]
72. Simeoni, M.; Galloway, P.; O'neil, A.; Gilkes, R. A procedure for mapping the depth to the texture contrast horizon of duplex soils in south-western Australia using ground penetrating radar, GPS and kriging. *Aust. J. Soil Res.* **2009**, *47*, 613–621. [CrossRef]
73. Gómez-Ortiz, D.; Pereira, M.; Martín-Crespo, T.; Rial, F.I.; Novo, A.; Lorenzo, H.; Vidal, J.R. Joint use of GPR and ERI to image the subsoil structure in a sandy coastal environment. *J. Coast. Res.* **2009**, *56*, 956–960.
74. Araújo, R.F.; Oliva, P.A.C.; Gomes, K.P.; Correia, K.A.; Pena, R.T.; da Silva, R.P. Application of geophysical tools for evaluation of adequate ponds for Aquaculture. In Proceedings of the 82nd EAGE Annual Conference & Exhibition, EAGE, Amsterdam, The Netherlands, 18–21 October 2021. Paper Number 3068. [CrossRef]
75. Shafi, J.; Waheed, K.N.; Mirza, Z.S.; Zafarullah, M. Assessment of soil quality for aquaculture activities from four divisions of Punjab, Pakistan. *J. Anim. Plant Sci.* **2021**, *31*, 556–566. [CrossRef]
76. Saraswathy, R.; Ravisankar, T.; Ravichandran, P.; Vimala, D.D.; Jayanthi, M.; Muralidhar, M.; Manohar, C.; Vijay, M.; Santharupan, T.C. Assessment of soil and source water characteristics of disused shrimp ponds in selected coastal states of India and their suitability for resuming aquaculture. *Indian J. Fish.* **2016**, *63*, 118–122. [CrossRef]
77. Gul, N.; Mussaa, B.; Masood, Z.; UR-Rehman, H.; Ullah, A.; Majeed, A. Study of Some Physiochemical Properties of Soil in Fish Pond at Circuit House, District Sibi of Province Balochistan, Pakistan. *Glob. Vet.* **2015**, *14*, 362–365. [CrossRef]
78. Arnold, W.S.; White, M.V.; Norris, H.A.; Berrigan, M.E. Hard clam (*Mercenaria* spp.) aquaculture in Florida, USA: Geographic information system applications to lease site selection. *Aquac. Eng.* **2000**, *23*, 203–231. [CrossRef]
79. Nayak, A.K.; Kumar, P.; Pant, D.; Mohanty, R.K. Land suitability modelling for enhancing fishery resource development in Central Himalayas (India) using GIS and multi-criteria evaluation approach. *Aquac. Eng.* **2018**, *83*, 120–129. [CrossRef]
80. Abdullah, R.; Mustafa, F.B.; Bhassu, S.; Azhar, N.A.A.; Bwadi, B.E.; Ahmad, N.S.B.N.; Ajeng, A.A. Evaluation of water and soil qualities for giant freshwater prawn farming site suitability by using the AHP and GIS approaches in Jebebu, Negeri Sembilan, Malaysia. *AIMS Geosci.* **2021**, *7*, 507–528. [CrossRef]
81. Francisco, H.R.; Corrêa, A.F.; Feiden, A. Classification of Areas Suitable for Fish Farming Using Geotechnology and Multi-Criteria Analysis. *ISPRS Int. J. Geo-Inf* **2019**, *8*, 394. [CrossRef]
82. Aghmashhadi, A.H.; Azizi, A.; Hoseinkhani, M.; Zahedi, S.; Cirella, G.T. Aquaculture Site Selection of *Oncorhynchus Mykiss* (Rainbow Trout) in Markazi Province Using GIS-Based MCDM. *ISPRS Int. J. Geo-Inf* **2022**, *11*, 157. [CrossRef]
83. Esmailpour-Poodeh, S.; Ghorbani, R.; Hosseini, S.A.; Salmanmahiny, A.; Rezaei, H.; Kamyab, H. A multi-criteria evaluation method for sturgeon farming site selection in the southern coasts of the Caspian Sea. *Aquaculture* **2019**, *513*, 734416. [CrossRef]
84. Laama, C.; Bachari, N.E.I. Evaluation of site suitability for the expansion of mussel farming in the Bay of Souahlia (Algeria) using empirical models. *J. Appl. Aquac.* **2018**, *31*, 1–19. [CrossRef]
85. Anand, A.; Krishnan, P.; Suryavanshi, A.S.; Choudhury, S.B.; Kantharajan, G.; Srinivasa Rao, C.; Manjulatha, C.; Babu, D.E. Identification of Suitable Aquaculture Sites Using Large-Scale Land Use and Land Cover Maps Factoring the Prevailing Regulatory Frameworks: A Case Study from India. *J. Indian Soc. Remote Sens.* **2021**, *49*, 725–745. [CrossRef]
86. Krupandan, A.G.; Gernez, P.; Palmer, S.; Thomas, Y.; Barillé, L. Exploring South African Pacific oyster mariculture potential through combined Earth observation and bioenergetics modelling. *Aquac. Rep.* **2022**, *24*, 101155. [CrossRef]
87. SIAGAS. Groundwater Information System-CPRM/Geological Survey of Brazil (SGB). 2021. Available online: <http://siagasweb.cprm.gov.br/layout/index.php> (accessed on 23 April 2021).
88. de Benedetto, D.; Montemurro, F.; Diacono, M. Repeated geophysical measurements in dry and wet soil conditions to describe soil water content variability. *Sci. Agric.* **2020**, *77*, 1–20. [CrossRef]
89. Zajíčková, K.; Chuman, T. Application of ground penetrating radar methods in soil studies: A review. *Geoderma* **2019**, *343*, 116–129. [CrossRef]
90. Campos, J.R.d.R.; Vidal-Torrado, P.; Modolo, A.J. Use of Ground Penetrating Radar to study spatial variability and soil stratigraphy. *Eng. Agrícola* **2019**, *39*, 358–364. [CrossRef]
91. Minet, J.; Verhoest, N.E.C.; Lambot, S.; Vanclooster, M. Temporal stability of soil moisture patterns measured by proximal ground-penetrating radar. *Hydrol Earth Syst. Sci.* **2013**, *10*, 4063–4097. [CrossRef]
92. Zhu, Q.; Lin, H.; Doolittle, J. Repeated electromagnetic induction surveys for determining subsurface hydrologic dynamics in an agricultural landscape. *Soil Sci. Soc. Am. J.* **2010**, *74*, 1750–1762. [CrossRef]
93. Taioli, F.; dos Santos, M.G.M.; Assine, M.L.; Mendes, D. How Ground Penetrating Radar helps to understand the Nhecolândia lakes landscape in the Brazilian Pantanal wetland. *Braz. J. Geol.* **2021**, *51*, 1–11. [CrossRef]
94. Xue, Y.; Tang, Z.; Hu, Q.; Drahota, J. Using the electromagnetic induction survey method to examine the depth to clay soil layer (Bt horizon) in playa wetlands. *J. Soils Sediments* **2020**, *20*, 556–570. [CrossRef]
95. Romero-Ruiz, A.; Linde, N.; Keller, T.; Or, D. A review of geophysical methods for soil structure characterization. *Rev. Geophys.* **2019**, *56*, 672–697. [CrossRef]

96. Wang, P.; Hu, Z.; Zhao, Y.; Li, X. Experimental study of soil compaction effects on GPR signals. *J. Appl. Geophys.* **2016**, *126*, 128–137. [[CrossRef](#)]
97. Muñoz, E.; Shaw, R.K.; Gimenez, D.; Williams, C.A.; Kenny, L. Use of ground-penetrating radar to determine depth to compacted layer in soils under pasture. In *Digital Soil Morphometrics*; Hartemink, A., Minasny, B., Eds.; Springer: Cham, Switzerland, 2016; pp. 411–421. [[CrossRef](#)]
98. Peralta, N.R.; Costa, J.L.; Balzarini, M.; Angelini, H. Delineation of management zones with measurements of soil apparent electrical conductivity in the Southeastern Pampas. *Can. J. Soil Sci.* **2013**, *93*, 205–218. [[CrossRef](#)]
99. André, F.; Van Leeuwen, C.; Saussez, S.; Van Durmen, R.; Bogaert, P.; Moghadas, D.; de Rességuier, L.; Delvaux, B.; Vereecken, H.; Lambot, S. High-resolution imaging of a vineyard in south of France using ground-penetrating radar, electromagnetic induction and electrical resistivity tomography. *J. Appl. Geophys.* **2012**, *78*, 113–122. [[CrossRef](#)]
100. Loperte, A.; Satriani, A.; Bavusi, M.; Lapenna, V.; Dellungo, S.; Sabelli, R.; Gizzi, F.T. Geophysical prospecting in archaeology: Investigations in SantaVenera, south suburb of Poseidonia-Paestum, Campania, southern Italy. *J. Geophys. Eng.* **2011**, *8*, 23–32. [[CrossRef](#)]
101. Moral, F.J.; Terrón, J.M.; Silva, J.R.M. Delineation of management zones using mobile measurements of soil apparent electrical conductivity and multivariate geostatistical techniques. *Soil Tillage Res.* **2010**, *106*, 335–343. [[CrossRef](#)]
102. Amato, M.; Basso, B.; Celano, G.; Bitella, G.; Morelli, C.; Rossi, R. In situ detection of tree root distribution and biomass by multi-electrode resistivity imaging. *Tree Physiol.* **2008**, *28*, 1441–1448. [[CrossRef](#)]
103. Rubin, Y.; Hubbard, S.S. *Hydrogeophysics. Water Science and Technology Library*; Springer: Dordrecht, The Netherlands, 2006.
104. Corwin, D.L.; Plant, R.E. Applications of apparent soil electrical conductivity in precision agriculture. *Comput. Electron. Agric.* **2005**, *46*, 1–10. [[CrossRef](#)]
105. Petersen, H.; Fleige, H.; Rabbel, W.; Horn, R. Applicability of geophysical prospecting methods for mapping soil compaction variability of soil texture on farm land. *J. Plant Nutr. Soil Sci.* **2005**, *168*, 68–79. [[CrossRef](#)]
106. Hubbard, S.; Grote, K.; Rubin, Y. Mapping the volumetric soil water content of a California vineyard using high-frequency GPR ground wave data. *Lead. Edge* **2002**, *21*, 552–559. [[CrossRef](#)]
107. Pradipta, A.; Soupios, P.; Kourgialas, N.; Doula, M.; Dokou, Z.; Makkawi, M.; Alfarhan, M.; Tawabini, B.; Kirmizakis, P.; Yassin, M. Remote Sensing, Geophysics, and Modeling to Support Precision Agriculture—Part 2: Irrigation Management. *Water* **2022**, *14*, 1157. [[CrossRef](#)]

Disclaimer/Publisher’s Note: The statements, opinions and data contained in all publications are solely those of the individual author(s) and contributor(s) and not of MDPI and/or the editor(s). MDPI and/or the editor(s) disclaim responsibility for any injury to people or property resulting from any ideas, methods, instructions or products referred to in the content.